# Shear-Flow Transition: the Basin Boundary

Norman R. Lebovitz
Department of Mathematics
The University of Chicago
5734 S. University Ave., Chicago, IL 60637, USA
email: norman@math.uchicago.edu

**Abstract**

The basin of attraction of a stable equilibrium point is investigated for a dynamical system (W97) that has been used to model transition to turbulence in shear flows. The basin boundary contains a linearly unstable equilibrium point $X_{lb}$ which, in the self-sustaining scenario, plays a role in mediating the transition in that transition orbits cluster around its unstable manifold. However we find – for W97 with canonical parameter values – that this role is played not by $X_{lb}$ but rather by a periodic orbit also lying on the basin boundary. Moreover, it appears via numerical computations that all orbits beginning near $X_{lb}$ relaminarize. We offer numerical evidence that the parameter values of W97 are postcritical in the following sense: for some, subcritical parameter values, the basin boundary coincides with the stable manifold of $X_{lb}$ and only a subset of nearby orbits relaminarize, whereas for supercritical values the basin boundary is the union of two stable manifolds, one belonging to the periodic orbit and dominating the basin boundary, and the other belonging to $X_{lb}$ and detectable only as an edge separating relaminarizing orbits of different characters. The periodic orbit appears at the critical parameter value via a homoclinic connection. This further leads to a proposal for the structure of the 'edge of chaos' somewhat different from that which has previously been proposed.
MSC numbers:76D05, 76F20

## 1 Introduction

Experimentally, laminar shear flows undergo transition to turbulence when the relevant parameter, the Reynolds number $R$, exceeds a critical value $R_c$. Mathematically, when the Navier-Stokes equations are linearized about the laminar flow, the expected passage from stability to instability at $R_c$ is not found. This is the familiar conundrum that linear theory fails to predict the critical value $R_c$ (cf., for example, the introductory remarks in [8] for a fuller discussion). A resolution of this conundrum is that the stable, laminar point $O$ possesses a basin of attraction $B$ whose boundary $\partial B$ passes increasingly close to $O$ with

increasing $R$, so that perturbations that may be small by laboratory standards are large enough to transgress $\partial B$ for sufficiently large values of $R$.

This idea of describing the problem of shear flows in the language of dynamical-systems theory is an attractive one but has limitations when the model systems are confined to very low dimensions. The present work is nevertheless confined to models of very low dimensions. The motivations are (1) the impression that the nature of the basin of attraction is an important element in the theory, (2) the observation that very little is known about it and (3) the conviction that one needs to understand the basin and its boundary in low-dimensional systems before proceeding to high-dimensional systems. This is not a new idea. For example, a part of the basin boundary has been calculated and graphed for a two-dimensional model in [4], and its importance has been further highlighted in a discrete, dynamical system in [15]. In the present paper we consider the four-dimension model W97 (as described in [17]) and minor modifications of it.

Some results that may be relevant to higher-dimensional models and to the Navier-Stokes (NS) equations, discussed in more detail in §5, include the convoluted structure of the boundary, which implies that the functional form of a perturbation may be as important as its size; that the vicinity of $X_{lb}$ may not be the only place to seek transition; and that the tendency of the region complementary to the basin of attraction to extreme narrowness in some parts of phase space may help to explain the 'edge of chaos' ([14]) in terms of the more familiar invariant sets of dynamical-systems theory.

The plan of the paper is as follows. We describe the mathematical setting in §2. In §3 we present Waleffe's model together with diagrams of the boundary of the basin of attraction indicating the periodic orbit that lies on that boundary, and the relaminarization of orbits starting near $X_{lb}$. In §4 we reset the parameters in order to conduct a parametric study, finding a critical parameter value at which the lower-branch equilibrium point is joined on the basin boundary by a large periodic orbit via a homoclinic bifurcation. The concluding section, §5, is devoted to drawing from this study a proposed interpretation of the edge of chaos that is related to but not the same as that of [14], and to brief remarks on the results of this paper and their implications for further study.

# 2 Mathematical Setting

The Navier-Stokes (NS) equations possess a number of very simple solutions representing laminar shear flows (plane Couette and Poiseuille flow, pipe flow, etc.). When these partial-differential equations are modeled by a finite-dimensional system, the laminar flow can modeled by an equilibrium point of that system, which we'll take to be the origin of coordinates $O$. Almost all such finite-dimensional systems that have been studied take the form

$$\dot{x} = Ax + b(x), x \in R^n \tag{1}$$

satisfying certain conditions:

1. $A$ is a non-normal, stable matrix.
2. $b(x)$ is quadratic in $x$ and $\sum_{j=1}^{n} x_j b_j(x) = 0$.

This structure can be inferred by a Galerkin projection of the NS equations onto $n$ basis vectors, while taking mild liberties with the boundary conditions.

The stability condition on $A$ implies that its eigenvalues lie in the left half-plane and therefore that the origin $O$ is asymptotically stable. The basin of attraction $B$ of an asymptotically stable equilibrium point is the set with the property that any orbit through a point of $B$ tends to the equilibrium point as $t \to +\infty$. It is an open set invariant under the flow, in the sense that any solution beginning in $B$ remains in $B$ on its maximal interval of existence $(a, \infty)$. In some examples $a = -\infty$, though this is not inevitable. It's set-theoretic boundary $\partial B$ (if it has one) is likewise invariant in the same sense (it is worth noting here that other, more restrictive, meanings have been given to $\partial B$: cf [15] and §5 below). The latter is typically of relative measure zero so orbits that lie *on* $\partial B$ are rare but important since they lie just at the transition from the laminar flow toward something "more interesting." In particular, the threshold amplitude for transition, which has been a subject of some interest ([1],[2],[3],[9],[13],[18]), is the minimum distance from the origin to the basin boundary. We denote such a threshold point by $T$.

It plays a role in the self-sustaining process of shear turbulence as outlined by Waleffe et al ([11],[16],[17]). In this three-part process sustained turbulence is envisaged as consisting of streamwise rolls (part one) leading toward a streaky flow (part two) whose instability reinforces the streamwise rolls (part three). Figure 1 illustrates the first two parts of this process: a phase point starting near $T$ evolves toward the unstable equilibrium point $X_{lb}$, a surrogate for the streaky flow. If it lies just above the basin boundary – which coincides in this diagram with the stable manifold of $X_{lb}$ – it as captured by the unstable manifold of $X_{lb}$ and sent toward $S$, a surrogate for turbulence.

# 3 The model W97

This is a four-dimensional model which may be written

$$\dot{x}_1 = -\delta r_1 x_1 + \sigma_1 x_4^2 - \sigma_2 x_2 x_3, \tag{2}$$
$$\dot{x}_2 = -\delta r_2 x_2 + \sigma_2 x_3 + \sigma_2 x_1 x_3 - \sigma_4 x_4^2, \tag{3}$$
$$\dot{x}_3 = -\delta r_3 x_3 + \sigma_3 x_4^2, \tag{4}$$
$$\dot{x}_4 = -\left(\sigma_1 + \delta r_4\right) x_4 + x_4 \left(\sigma_4 x_2 - \sigma_1 x_1 - \sigma_3 x_3\right). \tag{5}$$

Here $\delta = 1/R$ where $R$ is the Reynolds number and the eight constants $r_1$ through $\sigma_4$ are all positive (In an earlier model, W95, $\sigma_1$ =0: see [16]). There are canonical values for these constants that we use (following [2]) in this section:

$$(\sigma_1, \sigma_2, \sigma_3, \sigma_4) = (0.31, 1.29, 0.22, 0.68)$$
$$(r_1, r_2, r_3, r_4) = (2.4649, 5.1984, 7.6729, 7.1289).$$

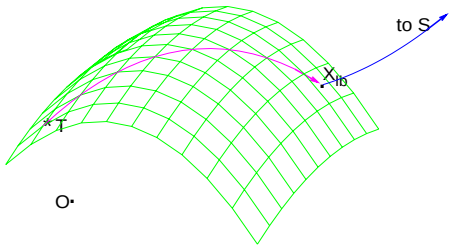


Figure 1: This cartoon illustrates Waleffe's picture: a part of the boundary $\partial B$ of the basin of attraction of the point $O$ is shown. The orbit shown begins at the threshold point $T$ and is attracted toward $X_{lb}$.

This system conforms to the rules (1) and (2) of model-building. It possesses the symmetry $S = \mathrm{diag}(1, 1, 1, -1)$ so a solution $x(t)$ has a companion solution $\tilde{x}(t)$ obtained by reversing the sign of $x_4(t)$ and the plane $x_4 = 0$ is an invariant plane. For these reasons there is no loss of generality in considering only solutions for which $x_4(t) \geq 0$. It is not difficult to show that the invariant plane $x_4 = 0$ lies entirely in $B$, the basin of attraction of the origin. It has been the subject of several studies (in addition to [2], see in particular that of [5]), with different goals from those emphasized here.

Two additional equilibrium solutions beyond that at the origin are found provided $\delta < \delta_{sn}$ or $R > R_{sn}$. With the choices for the parameters made above, $R_{sn} = 106.19$. The equilibrium solution lying closer in norm to the origin is called the"lower branch" $X_{lb}$, the one lying farther away is called the "upper branch" $X_{ub}$ (see Figure 2). The lower-branch solution is unstable, with a one-dimensional unstable manifold and a three dimensional stable manifold; the upper-branch solution may be stable or unstable, depending on the choices of $R$ and of the other parameters. For the values of $R$ considered in this paper and for the canonical values of the other parameters, $X_{ub}$ is asympotically stable. These equilibrium solutions are illustrated in Figure 2. The one marked $X_{lb}$ lies on $\partial B$. It is important to bear in mind, however, that $X_{lb}$ is by no means the closest point on that boundary to the origin. That closest point, denoted by $T$ in Figure 1, tends to the origin as $R \to \infty$ (cf. [2]) whereas $X_{lb}$ does not.

Figure (1) suggests that orbits starting on $\partial B$ tend toward $X_{lb}$, which mediates the transition. This will be so if the the stable manifold of $X_{lb}$ coincides with $\partial B$. This seems plausible (and has been found to be the case for some other models) but is by no means inevitable: the basin boundary and the stable manifold of $X_{lb}$ are both invariant sets for the system (2-5) but they are defined in different manners and need not be identical. In fact, we find that they are not identical for the model W97. The stable manifold of $X_{lb}$ is a proper subset

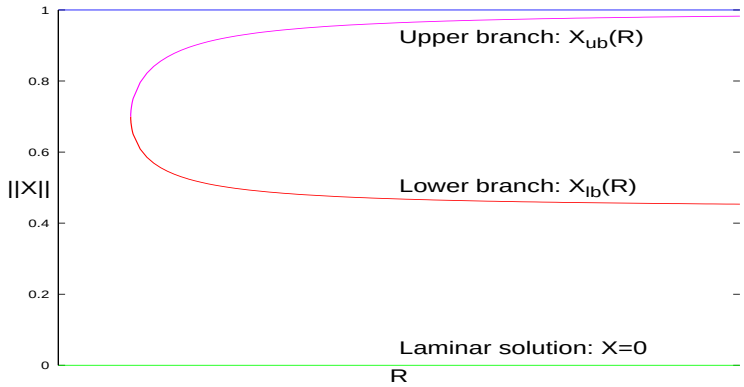


Figure 2: This is the diagram for equilibrium figures in Waleffe's model. The lower edge, where the norm $\|X\| = 0$, represents the laminar solution. The "lower branch" of further equilibrium solutions does not approach the laminar solution as $R \to \infty$ but instead tends to the indicated asymptote.

of $\partial B$, so a point on $\partial B$ lying far enough from $X_{lb}$ has a different evolution.

For W97 the threshold point $T$ has been located by Cossu ([2]). We find, by following orbits starting near $T$, that they are attracted not toward $X_{lb}$ but to a periodic orbit $P$ also lying on $\partial B$. We have thus far carried out calculations for $R = 145$ and $R = 190$ and we display only those for $R = 190$ (those for $R = 145$ are similar). We exploit Cossu's calculations to find refinements of the threshold values $T$: by repeated bisection we obtain a pair of values, $x_o$ and $x_i$ lying respectively just outside and just inside the basin of attraction $B$ and within a short distance $\epsilon$ of one another. It follows that there is a point $T$ on $\partial B$ within $\epsilon$ of either of them. We then find the structure of the basin boundary by calculating slices of it by two-dimensional hyperplanes (Figures 3, 4 and 5). $T$ lies close to the origin on the scales of these diagrams. That it does not lie *at* the origin is most easily seen in Figure 5.

We also obtain the orbit through $T = (T_1, T_2, T_3, T_4)$, finding the following. On taking $x_o$ as initial data, we find that after a transient of a few hundred units of time, the orbit is essentially periodic for many thousands of units of time, eventually spiraling into the stable, outside point $X_{ub}$; if $x_i$ is taken as the initial point a similar evolution is found except that at the end, the orbit tends to the laminar point $O$. Neither of these orbits comes close to $X_{lb}$.

In Figures (3), (4) and (5) two different kinds of objects are shown: slices of the basin boundary by two-dimensional hyperplanes on the one hand, and projections onto these hyperplanes of other features in the four-dimensional space (like the periodic orbit) on the other hand. The latter are indicated by single quotation marks.

While the self-sustaining process may be only slightly modified by replacing the equilibrium point $X_{lb}$ with the periodic orbit $P$ as the mediator of transition, the question of what role $X_{lb}$ plays in the dynamics now arises. We next turn

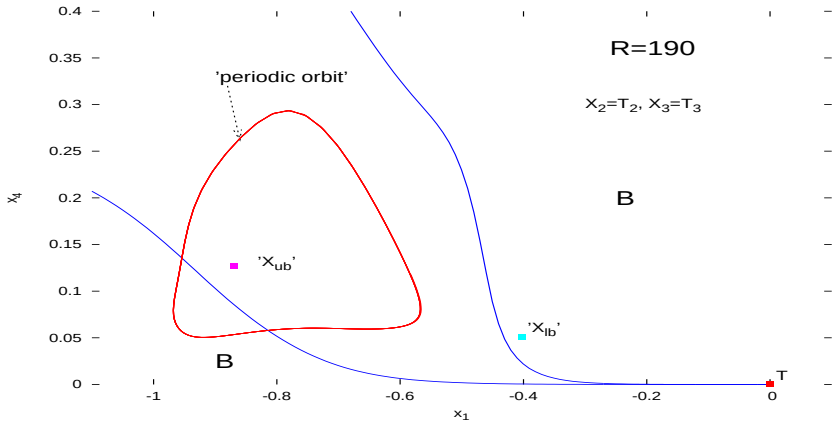


Figure 3: A region of the hyperplane $x_2 = T_2, x_3 = T_3$, which slices $\partial B$ in the indicated curves. The parts of this region lying in $B$ are so marked; the remainder lies outside. An orbit starting very near $T$ hovers near the periodic orbit, (the transient leading from $T$ to this orbit is not shown). The complementary region to the basin becomes very narrow near $T$ but is resolvable numerically.

to this.

The three-dimensional stable manifold of $X_{lb}$ coincides *locally* with $\partial B$. Denote by $\xi_t$ a unit vector transverse to $\partial B$ (for example, $\xi_t$ could have the unstable direction at $X_{lb}$). Then if for a scalar $v$ we choose initial data

$$x(0) = X_{lb} + v\xi_t \tag{6}$$

for a small value of $|v|$, we expect the orbit to depart from $X_{lb}$ along its unstable manifold. We anticipate that for one sign of $v$ the orbit will lie inside $B$ and for the other outside, and therefore that for one sign the orbit will tend to the origin and for the other will remain permanently outside the basin boundary, presumably tending for large $t$ to the stable equilibrium point at $X_{ub}$.

Instead, we find that all orbits tend to $O$, apparently echoing the persistent relaminarization found in other models ([7]). This is illustrated in Figure (6).

This violation of expectations could be explained by the following conjecture: $X_{lb}$ indeed lies on $\partial B$ but, near the part of $\partial B$ on which it lies, there is a second leaf of $\partial B$ exquisitely close to the first, and it's only for initial data in the narrow gap between the two leaves that orbits remain bounded away from the origin. That such narrow gaps are plausible for these systems may be seen by examining Figure (3) near the point $T$. In that case the gap, while narrow, is still easily detectable numerically. If this "gap conjecture" is correct for W97 with the canonical choice of parameters, the space between the two leaves is too small to be detected in the usual double precision arithmetic.

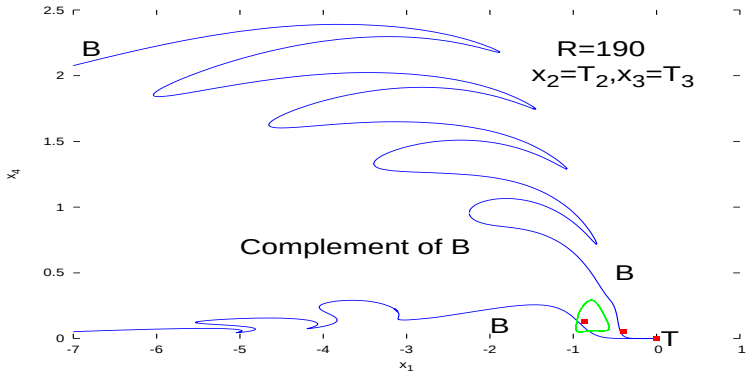


Figure 4: A global view of the preceding figure, showing more of the nature of the basin boundary, in the same slice as in Figure (3).

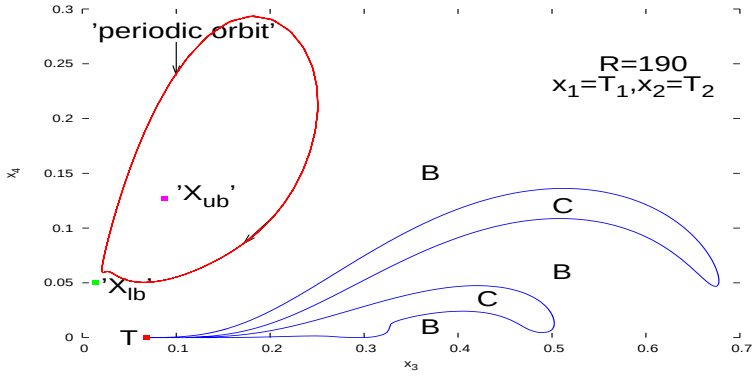


Figure 5: Like Figure (3), but a different slice.

# 4 A march toward relaminarization

We adopt a familiar strategy for testing this conjecture. We choose different parameters for which the problem simplifies and there is no violation of expectations, and make gradual changes in these parameters to see whether the more complicated situation encountered above unfolds. There is always some degree of arbitrariness in reparametrizing. The one we have chosen below is extreme and it is likely that a more modest reparametrization would suffice, although we have not explored this.

If we set all the positive constants in W97 equal to unity we find qualitative similarity to the case with canonical values for these constants. In particular, on choosing (say) $R = 100$, we find that all perturbations of $X_{lb}$ appear to relaminarize, as in Figure 6. The strategy will be to take all coefficients equal to unity with the exception of $\sigma_1$. An asymptotic analysis like that of [17] shows

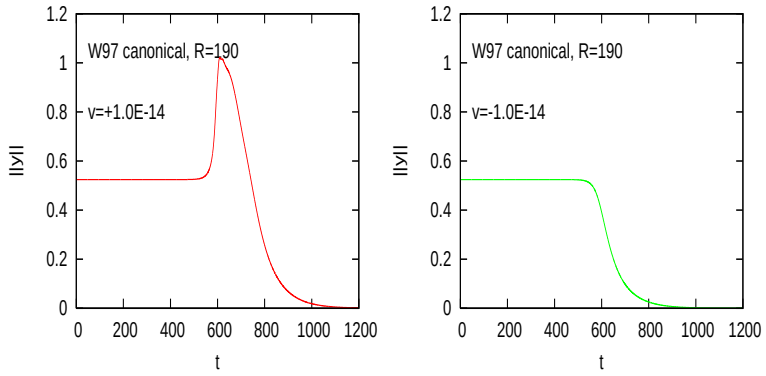


Figure 6: The model is W97 with the canonical values for the constants $r_1$ through $\sigma_4$ and $R = 190$. The norms of orbits are shown on the interval [0,1200] and $v = \pm 10^{-14}$. The two cases differ in the nature of the orbits and in the time for relaminarization to occur.

that, for small $\delta = 1/R$, the lower and upper branch equilibrium points are

$$X_{lb} \approx (-\frac{\sigma_1^2}{1+\sigma_1^2}, \frac{\sigma_1}{1+\sigma_1^2}, \sigma_1\delta, \sigma_1^{1/2}\delta)$$

and

$$X_{ub} \approx (-1+2\delta, \delta^{1/2}, \delta^{1/2}, \delta^{3/4}).$$

For small values of $\sigma_1$, we find numerically that there is a large and easily detectable gap near $X_{lb}$, i.e., in a description like that of Figure 6, orbits for which $v < 0$ relaminarize whereas those for which $v > 0$ do not. We then consider successively larger values of $\sigma_1$ to see if this gap gets successively narrower and ultimately becomes undetectable. In Figures 7 and 8, we show only slices of the basin boundary with the hyperplane $x_2 = X_{lb2}, x_3 = X_{lb3}$ since these seem to reveal the gap most clearly. The value of $R$ is held fixed at 15.

In these diagrams the region marked C, or Complement of B, is itself the basin of attraction of a stable periodic orbit lying outside B. The diagrams confirm the existence of a narrowing gap but reveal a further, unexpected feature: there appears to be a topological change in the nature of the basin boundary at precisely the parameter value at which the gap becomes suddenly undetectable, and is replaced by an 'edge', determined numerically by differences in time to relaminarize, as in Figure 6 above.

Simultaneous with the appearance of the edge is the appearance of a homoclinic loop, as indicated in Figure 8. This presages the appearance of a periodic orbit (P, say) lying on the basin boundary. This orbit is shown for a slightly post-critical value of $\sigma_1$ in Figure 9 in which it continues to have the appearance of a homoclinic loop. It is to be distinguished from the separate, stable periodic orbit attracting all orbits inside the complement of $B$. P has been detected in a numerical program designed to identify periodic orbits, which also confirms

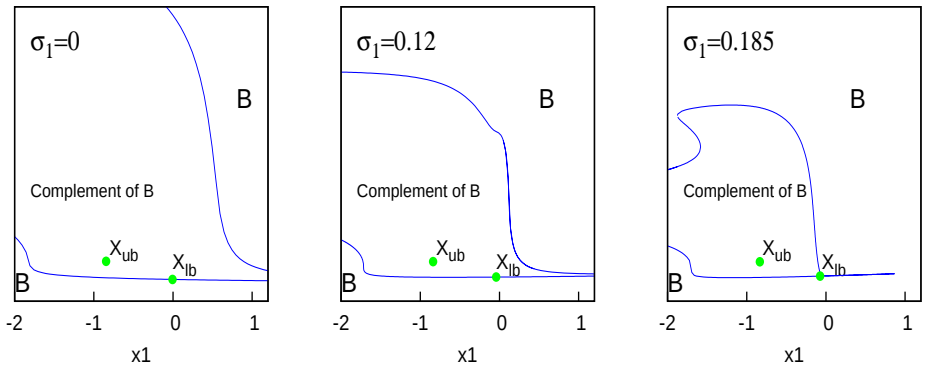


Figure 7: The ordinate is $x_4$. For each value of $\sigma_1$ shown, there is a progressively narrower gap to the right of $X_{lb}$. Orbits starting above the narrower gap require longer to relaminarize than those starting below. It looks on this scale as if the gap closes when $\sigma_1 = 0.185$, with $X_{lb}$ falling on a critical point. A close up of the region near $X_{lb}$ would show that this has not yet occurred for $\sigma_1 = 0.185$, but see Figure 8.

that it has one Floquet multiplier exceeding one in absolute value (i.e., of unstable type), and two less than one (the remaining multiplier equals one). This is consistent with the interpretation that its stable manifold now forms part of the basin boundary. That part of the basin boundary is robustly detectable as the borderline between orbits that tend to the origin and those that are captured by a stable periodic orbit. Similarly, in the case of canonical parameters depicted in Figures 3, 4 and 5, the part of the basin boundary consisting of the stable manifold of the periodic orbit is robust, and near-transition orbits are attracted to this.

# 5 Discussion

We have studied the modified system W97 in which all the constants except $\sigma_1$ have been set equal to one. The following sequence of statements is inferred from this study. Since the study is numerical, these statements are made subject to the usual caveats.

- When $\sigma_1$ is small enough, the boundary $\partial B$ of the basin of attraction $B$ of the origin coincides with the stable manifold $SM(X_{lb})$ of the unstable equilibrium point $X_{lb}$.
- When $\sigma_1$ exceeds a critical value, $\partial B$ is the union of two stable manifolds, $SM(X_{lb})$ and $SM(P)$, where $P$ is a periodic orbit that comes into existence via a homoclinic connection at the critical value of $\sigma_1$.
- Postcritically, $SM(X_{lb})$ is no longer detectable as the boundary between initial data whose orbits tend to the origin and those whose orbits are

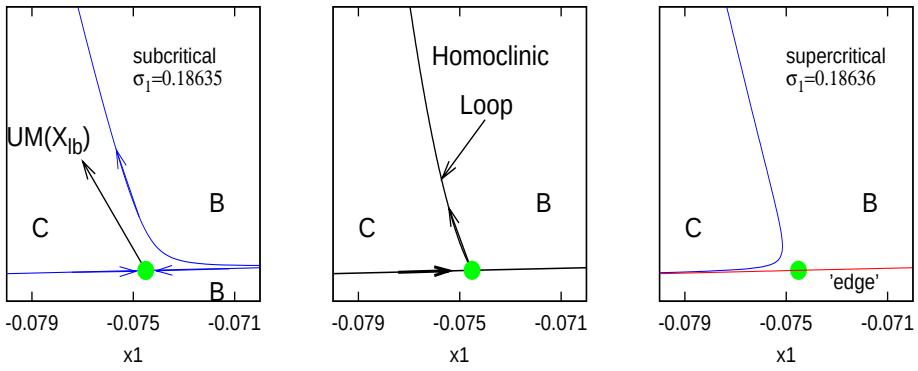


Figure 8: These are closeup views of the part of phase space near $X_{lb}$, which is represented by a large dot. The first and third of these diagrams are calculated but the central diagram is conjectural. The arrow marked $UM(X_{lb})$ in the left-hand diagram is the projection onto this hyperplane of the unstable direction at $X_{lb}$. It is tending toward tangency with the upper leaf of the stable manifold of $X_{lb}$, and thus forming the homoclinic connection (central diagram). The curve marked 'edge' in the third diagram divides long-time relaminarizations from short-time relaminarizations: no points of the complementary region C are detectable in the region of phase space immediately adjacent to this edge.

permanently bounded away from the origin, because *all* nearby orbits tend to the origin (relaminarize). It continues to be detectable as the dividing line between qualitatively different kinds of orbits, whose times to relaminarize are sharply different.

- Orbits through points on that part of $\partial B$ separating orbits that relaminarize from those that do not are all attracted to $P$, i.e., this part of $\partial B$ coincides with $SM(P)$.

Accepting these results from the modified version of W97, we can understand the results obtained in §3 for the canonical version of this model: the latter is postcritical in the sense that the homoclinic bifurcation has occurred along some path in parameter space leading from the modified parameters to their canonical values.

The sudden collapse of a part of the set complementary to the basin of attraction, as depicted in the right-hand diagram of Figure (8), is reminiscent of the 'edge of chaos' as described in [14] in that the line marked 'edge' is determined in a similar manner, namely, there is a sharp difference in relaminarization time for points just above and just below this line. A plausible interpretation of this edge is offerred in [14] along the following lines. In addition to the stable, laminar point at the origin of coordinates, there are two other invariant sets controlling the dynamics: a periodic orbit $P$ on the basin boundary and a chaotic saddle farther out in phase space (see their FIG. 3). Orbits beginning below $SM(P)$

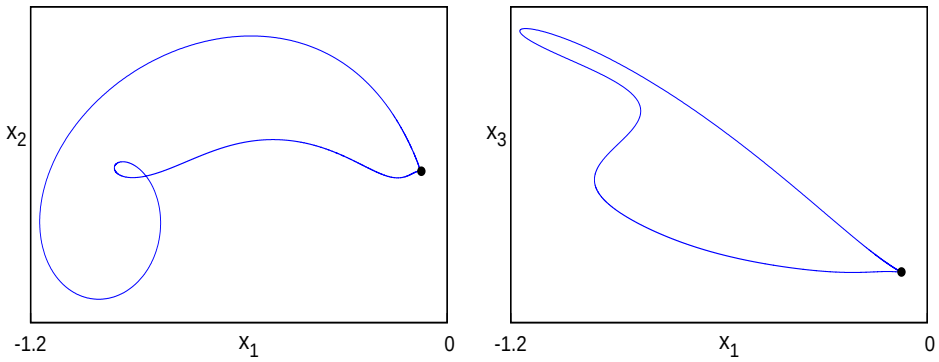


Figure 9: Two projections of the periodic orbit on $\partial B$ for a value of $\sigma_1 = 0.1865$, just post-critical. The dot represents $X_{lb}$, which appears on this scale to lie on the orbit, but in fact lies a small distance away from it.

tend directly to the origin, whereas those beginning above it first participate in the dynamics of the chaotic saddle before finally relaminarizing. This basic building block is then enhanced by intricate convolutions of $SM(P)$ to explain the repeated, sudden alterations in relaminarization times with distance along a line (see their FIG. 2).

In the model currently under consideration, the analog of their periodic orbit is the equilibrium point $X_{lb}$ and the analog of the chaotic saddle is a stable, periodic orbit lying farther out in phase space. Their basic building block is not plausible for the current model because of the stability of the invariant set farther out in phase space: orbits beginning above $SM(X_{lb})$ and visiting this orbit would be captured by it and not relaminarize. This suggests a picture of relaminarization like that of Figure (10), wherein the 'edge' consists of two leaves of $SM(X_{lb})$ so close together as to be numerically indistinguishable. This is close to the conjecture proposed in §3. It explains the longer relaminarization time of orbits beginning above $SM(X_{lb})$ by the need of such orbits to circumnavigate the basin of attraction of the stable, periodic orbit before relaminarizing. This set presents an obstacle to rapid relaminarization and is referred to as Obstacle in Figure 10. A diagram like FIG. 2 of [14] can then easily be envisaged as the result of intricate convolutions of $SM(X_{lb})$.

A number of issues for further study come to mind in view of the outcomes of the work reported here:

- A topological transition takes place in the structure of the basin boundary at the critical parameter value at which the periodic orbit $P$ appears. What is the nature of that transition? If the postcritical basin boundary is the union of the two stable manifolds $SM(P)$ and $SM(X_{lb})$, do these meet?

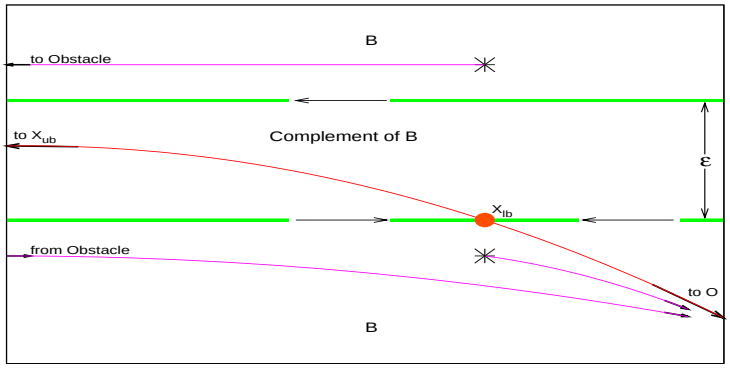


Figure 10: A conjecture regarding the 'edge.' The distance $\epsilon$ separating the top and bottom leaves of the basin boundary is so small as to escape numerical detection. If a point *could* be located between these leaves, it would ultimately be captured by a stable invariant set lying farther out in phase space and therefore be permanently bounded away from the origin. Attempts to locate such a point are frustrated by the narrowness of the gap, and will result instead in initial points indicated by the asterisks above and below. The orbit starting above is complicated but, since it is in $B$, ultimately decays to $O$. The orbit starting below decays more directly, and more quickly, to $O$.

- The structure of the basin boundaries makes it clear that whether a perturbation lies in $B$ or its complement depends not only on the amplitude of the perturbation but also – sensitively – on its direction in phase space (see for example Figure 3). Moreover, even for perturbations in the right direction to leave $B$, a large amplitude is not necessarily more effective than a smaller one. This must influence the experimental determination of the threshold for transition ([3]).

- In [15] the term 'basin boundary' is reserved for the set separating the basins of attraction of two, asymptotically stable invariant sets. This distinguishes the basin boundary from an 'edge set,' which may apply to a case when all invariant sets other than the origin are unstable. In the present paper we use the term 'basin boundary' to mean the set-theoretic boundary of the basin of attraction of the origin, irrespective of the stability character of any other invariant set. For all the parameter values considered in this paper, it turns out that there is indeed a second, asymptotically stable invariant set, but we nevertheless *also* find what appears to be an edge set. It seems important to clarify this fundamental distinction.

It is tempting to draw parallels with studies of numerical solutions of the Navier-Stokes equations, especially those for which periodic solutions emerge through a parametric study (e.g. [6], [10], [12]). However, given the range of models and of parameters employed in these studies on the one hand and the

obvious limitations of the model studied here on the other, such parallels would be highly speculative.

I wish to thank Carlo Cossu for generously sharing his data with me.

# References

[1] J.S. Bagget and L.N. Trefethen. Low-dimensional models of subcritical transition to turbulence. *Phys. Fluids*, 9:1043–1053, 1997.

[2] C. Cossu. An optimality condition on the minimum energy threshold in subcritical instabilities. *C. R. Mecanique*, 333:331–336, 2005.

[3] A.G. Darbyshire and T. Mullin. Transition to turbulence in constant-mass-flux pipe flow. *JFM*, 289:83–114, 1997.

[4] O. Dauchot and P. Manneville. Local versus global concepts in hydrodynamic stability theory. *Jour. Phys. II France*, 7:371–389, 1997.

[5] O. Dauchot and N. Vioujard. Phase space analysis of a dynamical model for the subcritical transition to turbulence in plane couette flow. *Eur. Phys. J. B*, 14:377–381, 2000.

[6] Y. Duguet, A.P. Willis, and R. Kerswell. Transition in pipe flow: the saddle structure on the boundary of turbulence. *JFM*, 613:255–274, 2008.

[7] B. Eckhardt. Turbulence transition in pipe flow: some open questions. *Nonlinearity*, 21:T1–T11, 2008.

[8] B. Eckhardt and A. Mersmann. Transition to turbulence in shear flow. *Phys. Rev. E*, 60(1):509–517, 1999.

[9] B. Hof, A. Juel, and T. Mullin. Scaling of the turbulence transition threshold in a pipe. *Phys. Rev. Lett.*, 91:244502, 2003.

[10] G. Kawahara and S. Kida. Periodic motion embedded in plane couette turbulence: regeneration cycle and burst. *JFM*, 449:291–300, 2001.

[11] J. Kim, J. Hamilton, and F. Waleffe. Regeneration mechanisms of near-wall turbulence structures. *JFM*, 287:317–348, 1995.

[12] M. Nagata. Three-dimensional finite-amplitude solutions in plane couette flow: bifurcation from infinity. *JFM*, 217:517–527, 1990.

[13] J. Peixinho and T. Mullin. Finite-amplitude thresholds for transition in pipe flow. *JFM*, 582:169–178, 2007.

[14] J.D. Skufca, J.A. Yorke, and B. Eckhardt. Edge of chaos in a parallel shear flow. *Phys. Rev. Lett.*, 96:174101, 2006.

[15] J. Vollmer, T.M. Schneider, and B. Eckhardt. Basin boundary, edge of chaos and edge state in a two-dimensional model. *New J. Phys.*, 11:013040, 2009.

[16] F. Waleffe. Hydrodynamic stability and turbulence: Beyond transients to a self-sustaining process. *Stud. Appl. Math.*, 95:319, 1995.

[17] F. Waleffe. On a self-sustaining process in shear flows. *Phys. Fluids*, 9(4):883–900, 1997.

[18] F. Waleffe and J. Wang. Transition threshold and the self-sustaining process. In T. Mullin and R. Kerswell, editors, *IUTAM Symposium on Laminar-Turbulent Transition and Finite Amplitude Solutions*, pages 85–106. Springer, 2005.